Crossover Behavior of the Anomalous Hall Effect and Anomalous Nernst Effect in Itinerant Ferromagnets

T. Miyasato,[1] N. Abe,[1] T. Fujii,[1] A. Asamitsu,[1,2] S. Onoda,[2,*] Y. Onose,[3] N. Nagaosa,[2,3,4] and Y. Tokura[2,3,4]

[1]*Cryogenic Research Center, University of Tokyo, Tokyo 113-0032, Japan*

[2]*Spin Superstructure Project, ERATO, JST, AIST Central 4, Tsukuba 305-8562, Japan*

[3]*Department of Applied Physics, University of Tokyo, Tokyo 113-8656, Japan*

[4]*Correlated Electron Research Center (CERC), AIST Central 4, Tsukuba 305-8562, Japan*

(Received 11 October 2006; published 24 August 2007)

The anomalous Hall effect (AHE) and anomalous Nernst effect (ANE) are experimentally investigated in a variety of ferromagnetic metals including pure transition metals, oxides, and chalcogenides, whose resistivities range over 5 orders of magnitude. For these ferromagnets, the transverse conductivity σ_{xy} versus the longitudinal conductivity σ_{xx} shows a crossover behavior with three distinct regimes in accordance qualitatively with a recent unified theory of the intrinsic and extrinsic AHE. We also found that the transverse Peltier coefficient α_{xy} for the ANE obeys the Mott rule. These results offer a coherent and semiquantitative understanding of the AHE and ANE to an issue of controversy for many decades.

DOI: 10.1103/PhysRevLett.99.086602 PACS numbers: 72.15.Eb, 72.20.Pa

The origin of the anomalous Hall effect (AHE) has long been an intriguing but controversial issue since the 1950s. Some of the theories explain the AHE from extrinsic origins such as skew-scattering ($\rho_{yx} \propto \rho_{xx}$) [1] or side-jump ($\rho_{yx} \propto \rho_{xx}^2$) [2] mechanisms due to the spin-orbit interaction.

In contrast to these extrinsic mechanisms, several works point out the intrinsic origin of the AHE, which is closely related to the quantal Berry phase on Bloch electrons in solids [3–7]: The intrinsic part of the anomalous Hall conductivity is given by the sum of the Berry-phase curvature of the Bloch wave function over the occupied states, in an analogy to the quantum-Hall effect. This Berry-phase scenario of the AHE has recently attracted much interest for its dissipationless and topological nature. Using first-principles band calculations, the intrinsic anomalous Hall conductivity has been calculated for ferromagnetic semiconductors [7,8], transition metals [9–11], and oxides [12,13], in quantitative agreement with experimental results. For example, the AHE in ruthenates ($SrRuO_3$) was found to be very sensitive to details of the electronic band structure such as the location of (nearly) crossing points of band dispersions. Such a momentum point acts as a ''magnetic monopole,'' yielding a large Berry-phase curvature and resulting in resonant enhancement of the anomalous Hall conductivity [12].

Recently, a theory of the AHE has been developed by taking into account this resonant contribution from the band crossing, where both the topological dissipationless current and the dissipative transport current are treated in the presence of the impurity scattering in a unified way [14]. It proposes three scaling regimes for the AHE as a function of the electron lifetime or the resistivity.

In this Letter, we experimentally study the anomalous Hall effect and anomalous Nernst effect in a variety of itinerant ferromagnets at low temperatures, to test the various scenarios of the AHE and ANE and finally to obtain a coherent unified understanding of their origins. Our AHE measurements on pure metals (Fe, Co, Ni, and Gd films), oxides [$SrRuO_3$ crystals (SRO) [12] and $La_{1-x}Sr_xCoO_3$ crystals (LSCoO) [15]], and chalcogenide-spinel crystals ($Cu_{1-x}Zn_xCr_2Se_4$) [16] have revealed three different scaling regimes of the anomalous Hall conductivity σ_{xy} as a function of the longitudinal conductivity σ_{xx}, which is in good quantitative agreement with the unified theory of the AHE taking into account both intrinsic and extrinsic origins [14]. Besides, all of the data of σ_{xy} against σ_{xx} almost follow one curve for these materials, except in the extremely clean case. We have also examined the anomalous Nernst effect (the Nernst effect due to the spontaneous magnetization), which provides us with additional useful information on the low-temperature electronic state and the relevance to the Berry-phase scenario of the AHE.

We used thin films of Fe, Co, Ni, and Gd with the thickness of 1 μm and the purity of 99.85%, 99.9%, 99+%, and 99.9%, respectively. Single crystals of $La_{1-x}Sr_xCoO_3$ ($x = 0.17$, 0.25, and 0.30) and $SrRuO_3$ were grown by a floating-zone method and a flux method, whose Curie temperatures are 120, 225, 235, and 160 K, respectively. Hall resistivity ρ_{yx} was measured by a 6-wire method using a physical properties measurement system (Quantum Design Co., Ltd.) together with the longitudinal resistivity ρ_{xx} as a function of magnetic field (H) and temperature (T). Transverse thermopower $Q_{yx} = E_y/\partial_x T$ was measured using the same platform by introducing necessary wirings. We apply a temperature gradient $\partial_x T$ to an electrically isolated sample in a magnetic field and measure the transverse voltage that appears. According to the linear transport theory, we have $\vec{j} = \tilde{\sigma}\vec{E} + \tilde{\alpha}(-\vec{\nabla}T)$ and $\vec{E} = \tilde{\rho}\vec{j} + \tilde{Q}\vec{\nabla}T$, where $\vec{j}$ stands for the electric current and $\vec{E}$ for the electric field, and $\tilde{\sigma}$, $\tilde{\rho}$, $\tilde{\alpha}$, and $\tilde{Q}$ denote

conductivity, resistivity, Peltier, and thermoelectric tensors, respectively. Then we obtain $Q_{xy} = -E_y/\partial_x T + Q_{xx}(\partial_y T/\partial_x T)$ as $\vec{j} = \vec{0}$. Because we confirmed that the second term is negligibly small compared to the first term, we defined $Q_{xy} = -E_y/\partial_x T$ in the following. The anomalous contribution in ρ_{yx} and Q_{xy} was determined by extrapolating ρ_{yx} and Q_{xy} vs H curves to $H = 0$. The transverse conductivity σ_{xy} was estimated as $-\rho_{xy}/\rho_{xx}^2$ and the transverse Peltier coefficient α_{xy} as $(Q_{xy} - Q_{xx}\tan\theta_{xy})/\rho_{xx}$, where θ_{xy} is the Hall angle. The contribution from magnetoresistance or magnetothermopower was carefully removed by subtracting $\rho_{yx}(-H)$ from $\rho_{yx}(H)$ or $Q_{xy}(-H)$ from $Q_{xy}(H)$.

Figure 1 shows the temperature dependence of anomalous Hall conductivity σ_{xy} in pure metals [upper panel, (a)] and oxides [lower panel, (b)]. Note that the scale of the vertical axis in Fig. 1(a) is logarithmic of $|\sigma_{xy}|$, while it is linear in Fig. 1(b). All of the ferromagnets studied are metallic except LSCoO ($x = 0.17$) as shown in the inset in Fig. 1. In oxides, the change of σ_{xy} is very complicated due to the change of M and even shows the sign change in SRO and LSCoO. Therefore, for oxides, to discuss only the influence of scattering events on the AHE, we need to concentrate on the lowest-temperature (5 K) data. In pure metals, the value of $|\sigma_{xy}|$ is almost constant and of the order of 100–1000 S/cm below room temperature down to

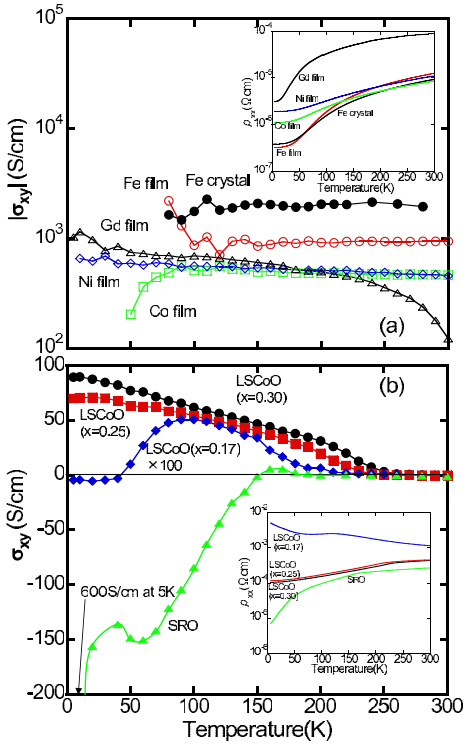

FIG. 1 (color online). Temperature dependence of anomalous Hall conductivity σ_{xy} for (a) pure metals in logarithmic scale and (b) oxides in linear scale. In the top panel, σ_{xy} is a negative quantity for Ni and Gd. The temperature dependence of longitudinal resistivity ρ_{xx} is also shown in the inset.

100 K, where the magnetization M is almost saturated (not shown), though the resistivity is still changing. This suggests that the mechanism of the AHE in this region does not depend on scattering events and is determined by the intrinsic Berry-phase mechanism.

Note that, for Fe and Co, it is difficult to reliably separate the anomalous Hall conductivity from the ordinary at such low temperatures as $\rho_{xx} < 10^{-6}$ Ω cm. Because of their small remnant magnetizations, the anomalous Hall resistivity ρ_{yx}^a should be estimated by separating it from the ordinary $\rho_{yx}^n = R_0 H$ at the applied magnetic field $H =$ 3 T, which is required to align the magnetic domain walls. This analysis becomes particularly important when ρ_{xx} becomes quite low as for Fe and Co at low temperatures. This is because $\rho_{yx}^n = R_0 H$, which is independent of ρ_{xx}, becomes comparable to ρ_{yx}^a, which is expected to decay with decreasing ρ_{xx}. For Fe and Co, we could safely determine R_0 at 80 and 50 K, respectively. In fact, this analysis is justified when the relaxation rate $1/\tau$ is much less than the cyclotron frequency ω_c at 3 T, since in this case the electrons are almost free from the Landau-level formations leading to the nonlinear H dependence, and we can use the linear H dependence of ρ_{yx}^n at this magnetic field. This gives a criterion of the value of ρ_{xx} for the present analysis as $\rho_{xx} \sim ha/e^2 E_F \tau \gg (ha/e^2) \times (\omega_c/E_F) \sim 10^{-7}$ Ω cm, with the Fermi energy E_F and the lattice constant a. For safety, we adopted only the data with $\rho_{xx} > 10^{-6}$ Ω cm.

Now we reveal a striking relation among various σ_{xy} values. Figure 2 shows the variation of the absolute value $|\sigma_{xy}|$ against the longitudinal conductivity σ_{xx} over 4 orders of magnitude in the ground state of itinerant ferromagnets. The data for $Cu_{1-x}Zn_xCr_2Se_4$ are also included in the figure. For pure metals, all data of $|\sigma_{xy}|$ shown in Fig. 1(a) are also plotted. The variation of $|\sigma_{xy}|$ can be categorized into three regions. (i) In the dirty regime with $\sigma_{xx} < 10^4$ S/cm, such as in $Cu_{1-x}Zn_xCr_2Se_4$ and $La_{1-x}Sr_xCoO_3$, the dependence of σ_{xy} on the residual resistivity is well described by $\sigma_{xy} \propto \sigma_{xx}^{1.6}$ experimentally.

(ii) In the intermediate region with $\sigma_{xx} =$ 10^4–10^6 S/cm, such as in pure metals and $SrRuO_3$, one can see that $|\sigma_{xy}|$ is nearly constant ($\simeq 1000$ S/cm), which means that $\rho_{yx} \propto \rho_{xx}^2$. This suggests that the extrinsic skew-scattering contribution has already decayed in this regime. Furthermore, this constant value of $|\sigma_{xy}|$ is consistent with the "resonant" AHE which gives the intrinsic contribution of the order of $e^2/ha \sim 10^3$ S/cm [14]. It is well known that the extrinsic side-jump contribution also yields a constant behavior of σ_{xy}. However, from the theoretical viewpoint, it is much smaller than e^2/ha, because of an additional factor ε_{SO}/E_F [14]. Therefore, we can safely remark that the σ_{xy} in the plateau region is dominated by the resonant intrinsic Berry-phase contribution. Note that if $|\sigma_{xy}|$ in the plateau region was much less than 10^3 S/cm, it could not be distinguished from the side-jump contribution.

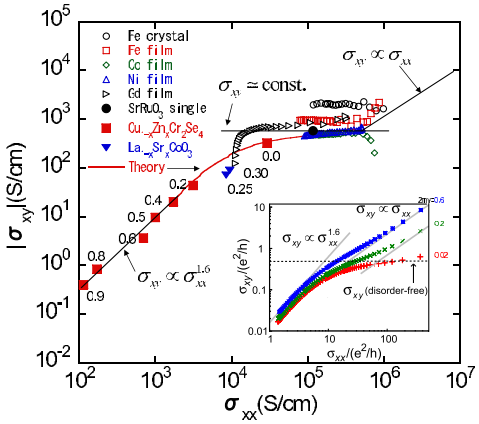

FIG. 2 (color online). Absolute value of anomalous Hall conductivity $|\sigma_{xy}|$ as a function of longitudinal conductivity σ_{xx} in pure metals (Fe, Ni, Co, and Gd), oxides ($SrRuO_3$ and $La_{1-x}Sr_xCoO_3$), and chalcogenide spinels ($Cu_{1-x}Zn_xCr_2Se_4$) at low temperatures. The three lines are $\sigma_{xy} \propto \sigma_{xx}^{1.6}$, $\sigma_{xy} = \text{const}$, and $\sigma_{xy} \propto \sigma_{xx}$ for the dirty, intermediate, and clean regimes, respectively. The inset shows theoretical results obtained from the same analysis as in Fig. 4 of Ref. [15] but for $E_F = 0.9$; $2m\upsilon = 0.02$ (+), 0.2 (×), and 0.6 (*). Here m is the effective mass, and υ is the strength of the δ-functional impurity potential. The theoretical curve for $2m\upsilon = 0.02$, after multiplying it by a factor $e^2/ha \sim 10^3$ S/cm, is also shown in comparison with the experimental results.

(iii) Finally, in the extremely conducting case with $\sigma_{xx} \simeq 10^6$ S/cm as in Fe and Co at low temperatures, $|\sigma_{xy}|$ does not remain constant any longer but depends on compounds. It is apparent that, in Fe, σ_{xy} tends to increase rapidly and that, in Co, $|\sigma_{xy}|$ shows a steep decrease because of the sign change of σ_{xy} from negative to positive at low temperatures. This gives another crossover from the intrinsic to the extrinsic region around $\sigma_{xx} \sim 10^6$ S/cm. It is most likely that there appears the extrinsic skew-scattering contribution to the AHE in this region, since it is expected to diverge as $\sigma_{xy} \propto \sigma_{xx}$ in the clean limit. As we mentioned above, however, a reliable analysis of the AHE in Fe and Co at further lower temperatures is difficult at the present stage, and the experimental determination of the scaling exponent in such extremely conducting cases would require further studies. Therefore, only the deviation from the plateau has meaning in the present analysis.

The above crossover behavior among the three scaling regimes is well understood by a unified theory of the AHE taking into account both intrinsic and extrinsic origins [14]: Three scaling regimes have been found for a generic two-dimensional model containing the resonant enhancement of σ_{xy} due to an anticrossing of band dispersions and the impurity scattering. The extrinsic skew-scattering mechanism gives the leading contribution in the extremely clean case, where the relaxation rate τ^{-1} is smaller than $2m\upsilon\varepsilon_{\text{so}}$, with the effective mass m, the impurity potential strength υ of the δ-functional form, and the spin-orbit interaction energy ε_{so}. This yields the scaling $\sigma_{xy} \propto \sigma_{xx}$. If the Fermi level is located around the anticrossing of band dispersions, a crossover to the intrinsic regime occurs around $\tau^{-1} \sim 2m\varepsilon_{\text{so}}$, with the resonant enhancement $\sigma_{xy} \sim e^2/h$ and the scaling $\sigma_{xy} = \text{constant}$. For the dirty regime with $\tau^{-1} > E_F$, there occurs another scaling $\sigma_{xy} \propto \sigma_{xx}^{1.6}$ [17]. The present experimental results on the crossover in σ_{xy} among the clean, intermediate, and dirty cases is thus well reproduced by this theory as shown in Fig. 2 as well as the inset.

Now we move on to the anomalous Nernst effect. The transverse Peltier coefficient α_{xy} is given by the Mott rule

$$\alpha_{xy} = \left(\frac{\pi^2 k_B^2}{3e}\right) T \frac{d}{d\epsilon}[\sigma_{xy}(\epsilon)]_{\mu}, \tag{1}$$

where k_B is the Boltzmann constant, e the elementary charge, and μ the chemical potential [18]. In Fig. 3, we show α_{xy} and M simultaneously in $La_{1-x}Sr_xCoO_3$ ($x = 0.3$, 0.25, and 0.17) and $SrRuO_3$. All of the materials (not shown for pure metals) seem to show qualitatively very similar temperature dependence that α_{xy} starts to increase just below T_C, being almost proportional to M, then decreases at low temperatures linearly with T, and finally vanishes toward absolute zero. These behaviors are well understood using the above formula: α_{xy} just below T_C is subject to the factor $(d\sigma_{xy}/d\epsilon)_{\mu}$, where the modification of the band structures at the Fermi level takes place due to the ferromagnetic transition. After the saturation of M, the T-linear term becomes dominant in the change of α_{xy}.

In order to confirm the validity of Eq. (1) further, we performed a quantitative analysis on α_{xy} in LSCoO($x = 0.3$–0.18). The equation is rewritten to

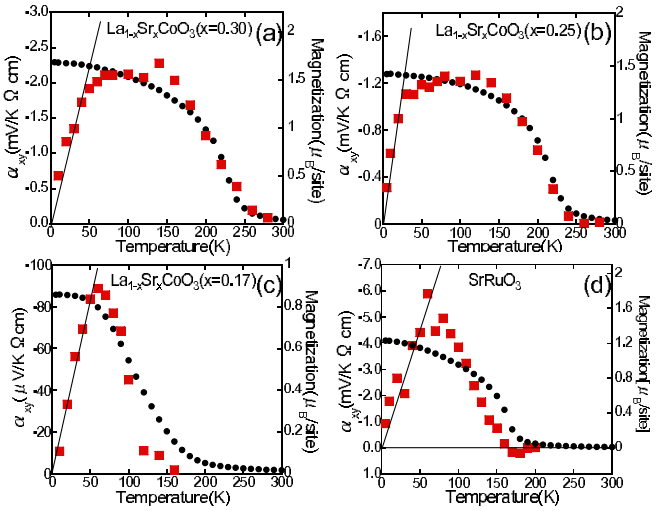

FIG. 3 (color online). Temperature dependence of anomalous transverse Peltier coefficient α_{xy} (squares) and magnetization M (circles) in (a) $La_{1-x}Sr_xCoO_3$ ($x = 0.3$), (b) $La_{1-x}Sr_xCoO_3$ ($x = 0.25$), (c) $La_{1-x}Sr_xCoO_3$ ($x = 0.17$), and (d) $SrRuO_3$. The straight line at low temperatures represents T-linear variation of α_{xy}.

TABLE I. Experimental data of α_{xy}/T (μV/K$^2\,\Omega$ cm), σ_{xy} (S/cm) at a lowest temperature (5 K), carrier density n (10^{23}/mol) derived from the ordinary Hall effect at room temperature, and electronic heat-capacity coefficient γ (mJ/mol K^2) in $La_{1-x}Sr_xCoO_3$. The LHS in Eq. (2) is the average of two successive α_{xy}/T, and the RHS is estimated using the average of γ and the difference $\Delta\sigma_{xy}/\Delta n$.

x	α_{xy}/T	LHS	RHS	σ_{xy}	n	γ
0.30	−437			90.3	1.43	49.1
		−285	−339			
0.26	−132			34.2	1.89	39.5
		−142	−170			
0.22	−153			23.8	2.04	41.1
		−85.9	−103			
0.18–2	−19.2			1.10	2.86	19.0
		−27.8	−8.77			
0.18–1	−8.62			−0.002	3.27	32.4

$$\frac{\alpha_{xy}}{T} = \frac{\gamma}{e}\frac{d}{dn}[\sigma_{xy}(\epsilon)]_\mu, \tag{2}$$

with the electronic heat-capacity coefficient γ by using the transformation $\frac{d}{d\epsilon}[\sigma_{xy}(\epsilon)]_\mu = \frac{dn}{d\epsilon}\frac{d}{dn}[\sigma_{xy}(\epsilon)]_\mu$. We obtained γ from heat-capacity measurement and the carrier density n from the ordinary Hall effect at 300 K, which is far above T_C. These values are shown in Table I. Because the composition x is nominal, we employed two samples with $x = 0.18$ showing different values of physical quantities [19]. The left-hand and right-hand sides (LHS and RHS, respectively) of Eq. (2) were estimated independently using these values in the center of Table I, replacing the differential $d\sigma_{xy}/dn$ with the difference $\Delta\sigma_{xy}/\Delta n$, and the relation of both sides was summarized in Fig. 4. The proportionality between these two quantities is obvious, and the slope is about 0.85 and slightly different from 1. Although we do not understand the reason for this slight discrepancy yet, α_{xy} obeys Eq. (2) quantitatively, and hence the thermoelectric Hall transport property is understandable, at least in the dirty case, in terms of the Mott rule. This may suggest that the Berry-phase contribution to the thermoelectric Hall transport phenomena is dominant mainly through σ_{xy}.

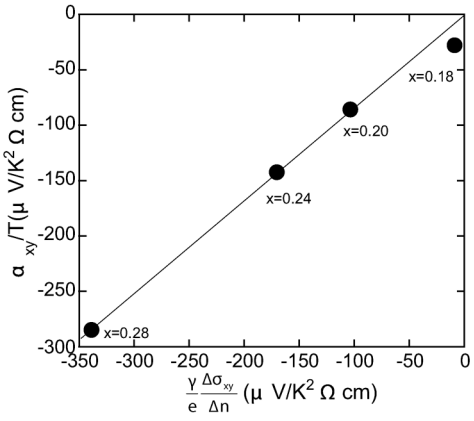

FIG. 4. The relation between the left-hand and right-hand sides of Eq. (2) derived independently using the experimental data in Table I for $La_{1-x}Sr_xCoO_3$. The line has a gradient of about 0.85.

In summary, we have investigated the anomalous Hall effect and anomalous Nernst effect in various ferromagnetic metals, such as Fe, Co, Ni, Gd, $La_{1-x}Sr_xCoO_3$, $SrRuO_3$, and $Cu_{1-x}Zn_xCr_2Se_4$. The anomalous Hall conductivity σ_{xy} in the ground state shows three different behaviors against the longitudinal conductivity σ_{xx}, being almost independent of materials. These crossover behaviors can be well understood by a recent theory taking into account both intrinsic and extrinsic origins of the AHE. We have also shown that the relation between the anomalous Nernst effect and the anomalous Hall effect can be explained quantitatively by the Mott rule.

The authors thank N. P. Ong for useful comments on the separation of anomalous and ordinary Hall conductivities. This work was partly supported by the Grant-in-Aid for Scientific Research (No. 15104006, No. 16076205, No. 17105002, and No. 17038007) from the Ministry of Education, Culture, Sports, Science and Technology, Japan.

*Present address: RIKEN (The Institute of Physical and Chemical Research), Wako 351-0198, Japan.

[1] J. Smit, Physica (Amsterdam) **21**, 877 (1955); **24**, 39 (1958).
[2] L. Berger, Phys. Rev. B **2**, 4559 (1970).
[3] R. Karplus and J. M. Luttinger, Phys. Rev. **95**, 1154 (1954); J. M. Luttinger, Phys. Rev. **112**, 739 (1958).
[4] J. Ye *et al.*, Phys. Rev. Lett. **83**, 3737 (1999).
[5] M. Onoda and N. Nagaosa, J. Phys. Soc. Jpn. **71**, 19 (2002); Y. Taguchi *et al.*, Science **291**, 2573 (2001).
[6] Y. Lyanda-Geller *et al.*, Phys. Rev. B **63**, 184426 (2001).
[7] T. Jungwirth, Q. Niu, and A. H. MacDonald, Phys. Rev. Lett. **88**, 207208 (2002).
[8] C. Zeng *et al.*, Phys. Rev. Lett. **96**, 037204 (2006).
[9] J. G. Yao *et al.*, Phys. Rev. Lett. **92**, 037204 (2004).
[10] S. A. Baily and M. B. Salamon, Phys. Rev. B **71**, 104407 (2005).
[11] J. Kotzler and W. Gil, Phys. Rev. B **72**, 060412(R) (2005).
[12] Z. Fang *et al.*, Science **302**, 92 (2003); R. Mathieu *et al.*, Phys. Rev. Lett. **93**, 016602 (2004).
[13] L. M. Wang, Phys. Rev. Lett. **96**, 077203 (2006).
[14] S. Onoda, N. Sugimoto, and N. Nagaosa, Phys. Rev. Lett. **97**, 126602 (2006).
[15] Y. Onose and Y. Tokura, Phys. Rev. B **73**, 174421 (2006).
[16] W.-L. Lee *et al.*, Science **303**, 1647 (2004).
[17] This exponent is also expected in the "insulator" regime of quantum-Hall systems [L. P. Pryadko and A. Auerbach, Phys. Rev. Lett. **82**, 1253 (1999)].
[18] E. H. Sondheimer, Proc. R. Soc. London **193**, 484 (1948); L. Smrčka and P. Středa, J. Phys. C **10**, 2153 (1977).
[19] This doping level is close to the metal-insulator boundary in $La_{1-x}Sr_xCoO_3$ [15], and hence the properties are quite sensitive to slight off-stoichiometry.